Pure Appl. Geophys. 173 (2016), 3341–3356

DOI 10.1007/s00024-016-1263-6

Pure and Applied Geophysics

Kinematic 3-D Retro-Modeling of an Orogenic Bend in the South Limón Fold-and-Thrust Belt, Eastern Costa Rica: Prediction of the Incremental Internal Strain Distribution

CHRISTIAN BRANDES,[1] DAVID C. TANNER,[2] and JUTTA WINSEMANN[1]

Abstract—The South Limón fold-and-thrust belt, in the back-arc area of southern Costa Rica, is characterized by a 90° curvature of the strike of the thrust planes and is therefore a natural laboratory for the analysis of curved orogens. The analysis of curved fold-and-thrust belts is a challenge because of the varying structural orientations within the belt. Based on seismic reflection lines, we created a 3-D subsurface model containing three major thrust faults and three stratigraphic horizons. 3-D kinematic retro-deformation modeling was carried out to analyze the spatial evolution of the fold-and-thrust belt. The maximum amount of displacement on each of the faults is (from hinterland to foreland); thrust 1: 800 m; thrust 2: 600 m; thrust 3: 250 m. The model was restored sequentially to its pre-deformational state. The strain history of the stratigraphic horizons in the model was calculated at every step. This shows that the internal strain pattern has an abrupt change at the orogenic bend. Contractional strain occurs in the forelimbs of the hanging-wall anticlines, while a zone of dilative strain spreads from the anticline crests to the backlimbs. The modeling shows that a NNE-directed transport direction best explains the structural evolution of the bend. This would require a left-lateral strike-slip zone in the North to compensate for the movement and thereby decoupling the South Limón fold-and-thrust belt from northern Costa Rica. Therefore, our modeling supports the presence of the Trans-Isthmic fault system, at least during the Plio-Pleistocene.

Key words: Fold-and-thrust belt, kinematic modeling, active margin, Central America, Costa Rica, Cocos Ridge.

1. Introduction

Southern Central America is a complex Late Mesozoic/Cenozoic island-arc system. The Costa Rican part of the island arc can be subdivided into a northern and a southern arc segment (SEYFRIED *et al.* 1991). The southern Costa Rican arc segment is influenced by flat subduction of the Cocos Ridge (CORRIGAN *et al.* 1990; GARDNER *et al.* 2013), which results in deformation and uplift on the upper-plate forearc (MORELL *et al.* 2008, 2012) (Fig. 1). Early work on the bivergent southern Costa Rican land-bridge was carried out by GREB *et al.* (1996). The structural evolution of the forearc fold-and-thrust belt (Fila Costeña) has been comprehensively studied during the last decade (MENDE 2001; FISHER *et al.* 2004; SITCHLER *et al.* 2007; MORELL *et al.* 2008, 2012, 2013; GARDNER *et al.* 2013). The onshore and off-shore back-arc fold-and-thrust belt (South Limón belt) was analyzed by MENDE (2001) and BRANDES *et al.* (2007a, b, c; 2008); the latter focuses on basin dynamics (burial history and temperature evolution) and the architecture of the fold-and-thrust belt. An important structural feature in the area is the bend of the South Limón fold-and-thrust belt to the north-west, close to the city of Puerto Limón, where the strike of the thrusts changes through 90° (Fig. 2). This bend was first illustrated by PROTTI and SCHWARTZ (1994). BRANDES *et al.* (2007c) analyzed the sediment distribution on the offshore part of the South Limón fold-and-thrust belt and suggested that most of the deformation took place during the Pleistocene. Initial movements could have started already in the Late Pliocene (BRANDES *et al.* 2007c), but evidence is limited.

Kinematic evolution of fold-and-thrust belts is commonly analyzed in 2-D cross sections. The construction of 2-D balanced sections has evolved into a key technique in the analysis of contractional tectonics (e.g., DAHLSTROM 1969, 1990; COOPER and TRAYNER 1986; DEPAOR 1988; WU *et al.* 2005; TANNER *et al.* 2011). However, plane strain is typically

[1] Institut für Geologie, Leibniz Universität Hannover, Callinstraße, 30167 Hannover, Germany. E-mail: brandes@geowi.uni-hannover.de

[2] Leibniz Institute for Applied Geophysics (LIAG), Stilleweg 2, 30655 Hannover, Germany.

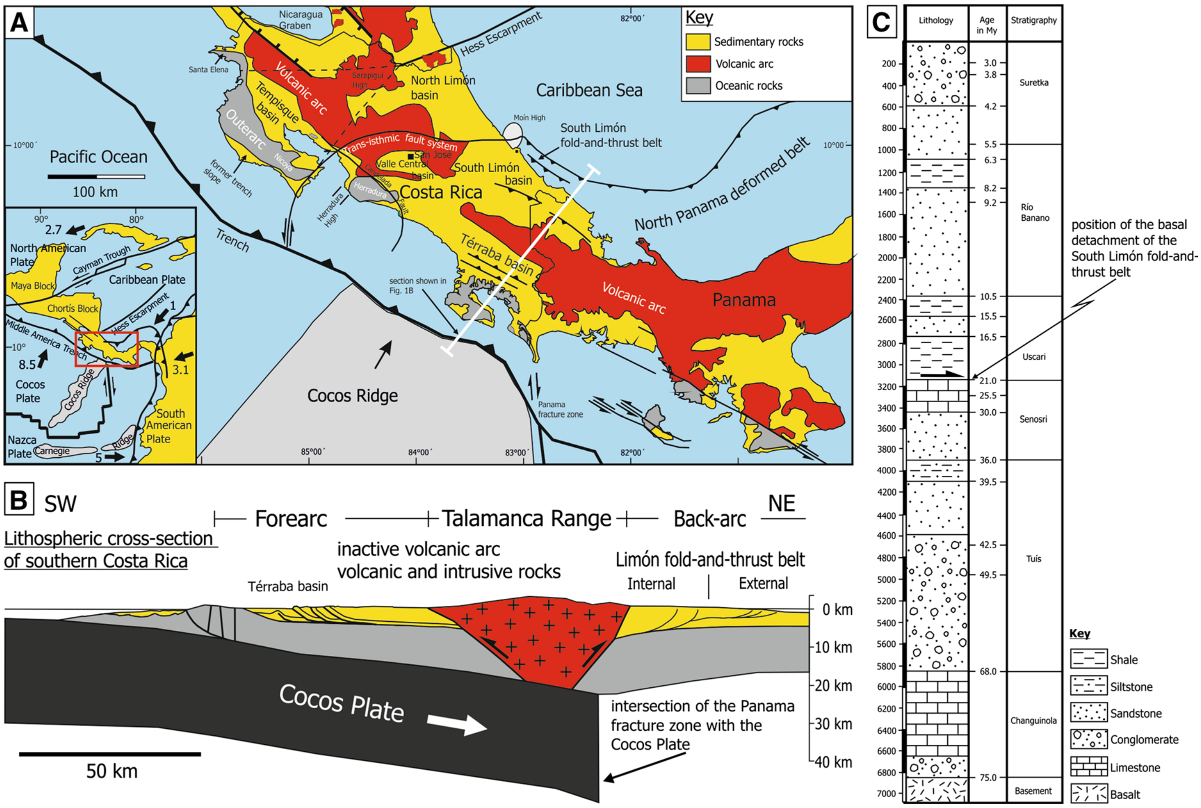

Figure 1

a Tectonic map of Costa Rica. The South Limón fold-and-thrust belt is located behind the island arc and extends along the southeastern Caribbean coast (modified after Barboza *et al.* 1997; Fernandez *et al.* 1997). The plate tectonic map of the Caribbean region (insert on the *left side*) is modified after Ross and Scotese (1988), Donnelly (1989), Meschede and Frisch (1998), and DeMets (2001). *Red box* shows location of detailed study area. Numbers are modern, absolute plate vectors (in cm year^{-1}). **b** Crustal-scale cross section of southern Costa Rica (modified after Fisher *et al.* 2004, Morell 2016) that shows the bivergent structure of the active margin. **c** Lithologic log of the South Limón Basin (modified after Campos 2001 and Brandes *et al.* 2008). The rheological contrast between the platform carbonates of the Senosri Formation and the overlying shales of the Uscari Formation defines the depth of the detachment of the South Limón fold-and-thrust belt

assumed. The analysis of fold-and-thrust belts in map view (e.g., Affolter and Gratier 2004) and 3-D (e.g., Tanner *et al.* 2003, Sala *et al.* 2014) also underwent considerable progress in the last decades. A 3-D approach integrates lateral geometric variations obtained from map and depth views into the cross section-based structural restoration (Tanner *et al.* 2003). According to Hindle and Burkhard (1999), only 3-D restoration of a curved fold-and-thrust belt can provide reliable information on true displacement and the amount of internal strain.

This study presents the 3-D structural analysis of the north-western bend of the South Limón fold-and-thrust belt, based on a 3-D model built from intersecting 2-D seismic reflection lines (Fig. 2). Our aim is to understand the kinematic evolution of the structure.

1.1. Salients, Oroclines and Syntaxes

Curved fold-and-thrust belts were recognized first by Suess (1908) and Argand (1924), and have been studied worldwide. In the context of curved fold-and-thrust belts, a specific terminology has been developed. The term salient is used to describe orogens that are convex to the foreland (Macedo and Marshak 1999; Fig. 3a). Salient development is controlled by the pre-deformation geometry of the sedimentary basin or the interaction of the fold-and-thrust belt with an indenter, strike-slip faults, or other

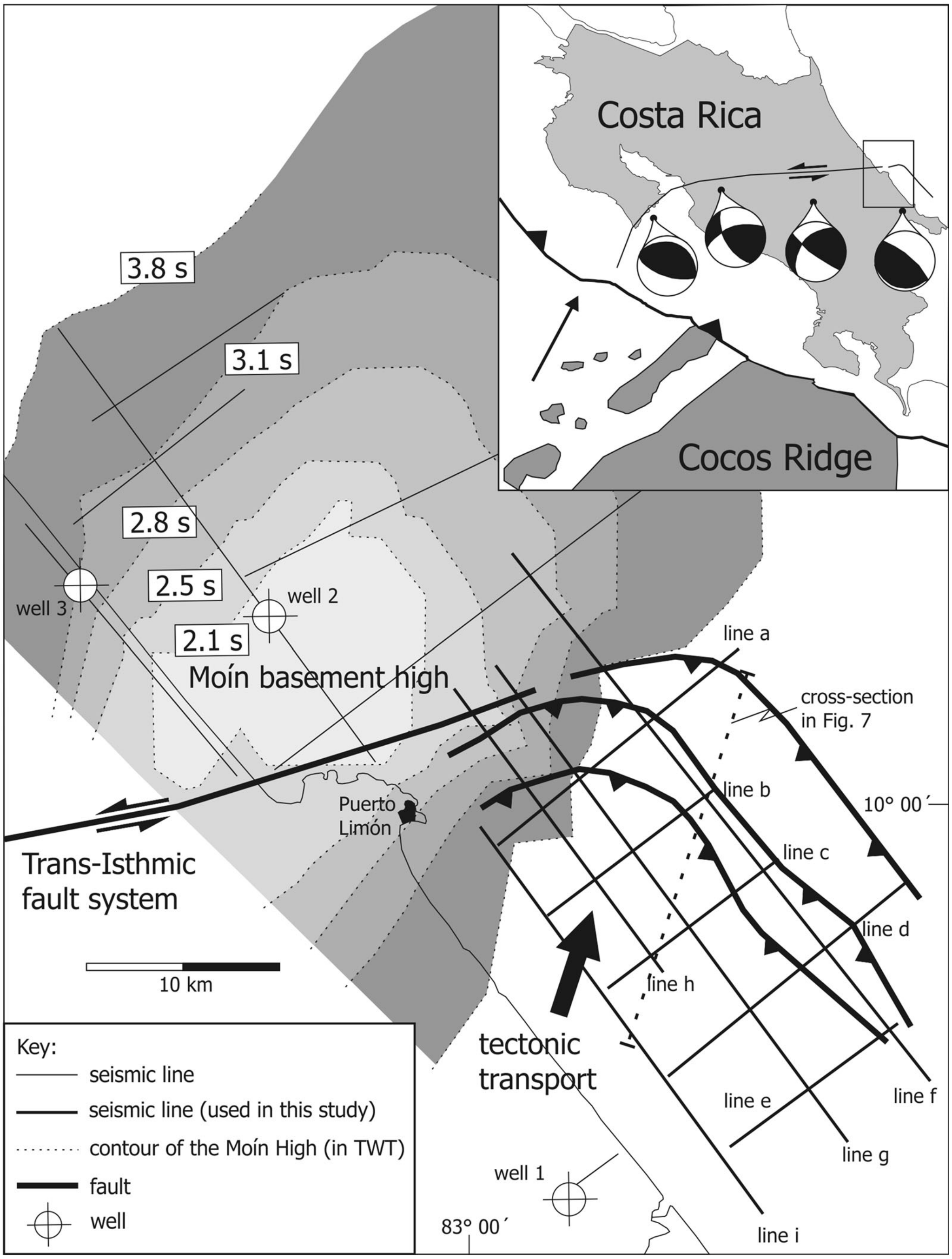

Figure 2
Seismic lines and well locations in the eastern coastal area of the Costa Rican back-arc. The *bold lines* indicate the locations of the seismic sections used in this study. The position and geometry of the Moín basement high is shown as isolines in two-way travel time (modified after Brandes *et al.* 2007a, b, c, 2009). The trace of the cross section in Fig. 7 is shown. The South Limón fold-and-thrust belt is closely related to the Moín basement high and the Trans-Isthmic fault system. Focal mechanisms of Marshall and Fisher (2000) imply strike-slip movements along the Trans-Isthmic fault system that transform into reverse movements in the area of the South Limón fold-and-thrust belt

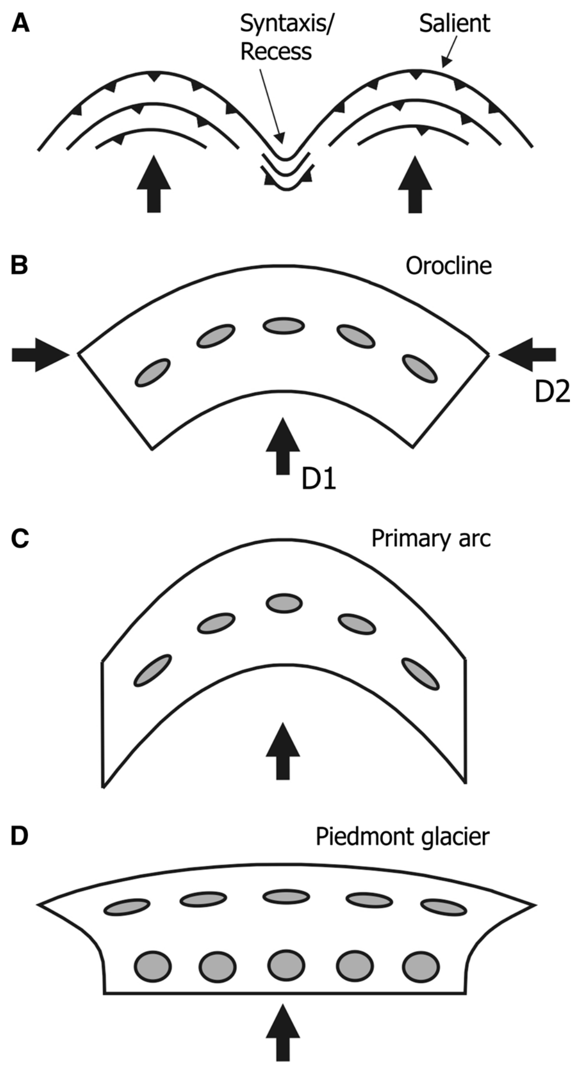

Figure 3
Conceptual models for curved fold-and-thrust belts. **a** The term salient is used to describe orogens that are convex to the foreland; a segment concave to the foreland is called a recess (based on Marshak 2004). **b** An orocline is an initially straight fold-and-thrust belt that was later bent. **c** Primary arc and **d** Piedmont glacier (after Hindle and Burkhard 1999). Primary arcs and Piedmont glaciers have different internal transport directions. In map view, primary arcs show uniform transport directions, whereas Piedmont glaciers have diverging transport directions

obstacles (Marshak 2004). A segment that is concave to the foreland is called a recess (van der Pluijm and Marshak 2004) (Fig. 3a). The transformation of an initially straight orogen front into a curved one is called oroclinal bending (Carey 1955, 1958). Oroclinal bending usually involves two deformation phases: the first creates the fold-and-thrust belt and the second bends it. A syntaxis is an abrupt bend in an otherwise geometrically straight orogen (Gates *et al.* 2004). Marshak (2004) used the term recess to describe a syntaxis (Fig. 3a).

Hindle and Burkhard (1999) divide curved fold-and-thrust belts into the three groups: *oroclines*, *primary arcs* and *Piedmont glaciers* (Fig. 3b–d). Strain within an orocline is constant along strike, as it is for a so-called Piedmont glacier; however, in the latter, strain increases toward the foreland. Within a primary arc, strain is concentrated at the edges of the fold-and-thrust belt. Based on Carey (1955, 1958), oroclines are defined as initially straight fold-and-thrust belts that were later modified by bending. Carey (1958) assumes that a fold-and-thrust belt initially forms under pure shear shortening, which is then followed by bending. Primary arcs and Piedmont glaciers can be distinguished on the basis of transport directions within the deforming wedge. In map view, primary arcs show uniform transport directions, whereas Piedmont glaciers have diverging transport directions Hindle and Burkhard (1999) (Fig. 3c, d).

The curvature of fold-and-thrust belts can be also explained in terms of either pure bending, radial thrusting, curve-parallel simple shear, uniform displacement/uniform shortening or transport-parallel simple shear, according to Ferrill and Groshong (1993).

2. *Geological Setting*

The geology of Central America is influenced by the interaction of the oceanic Cocos, Nazca, and Caribbean Plates, and the continental North and South American Plates (Fig. 1). The Cocos and Nazca Plates are remnants of the oceanic Farallon Plate. They are subducted beneath the Caribbean Plate along the NW–SE trending Central America trench. The present-day subduction velocity off Costa Rica, relative to the Caribbean Plate, is 8.5 cm $year^{-1}$ (DeMets 2001). The geological evolution of southern Costa Rica has been studied by many authors. Studies were carried out on many different topics, such as the arc-related sedimentary basins (Corrigan *et al.* 1990; Astrorga *et al.* 1991;

Seyfried *et al.* 1991; Amann 1993; Bowland 1993; von Eynatten *et al.* 1993; Campos 2001; Brandes *et al.* 2007a, b, c) and offshore geophysics (Ranero and von Huene 2000; Barckhausen *et al.* 2003) but detailed knowledge of the back-arc area and the related fold-and-thrust belts is still limited.

Southern Central America is characterized by the northeastward subduction of the Cocos Plate. An important feature of the Cocos Plate is the NE–SW-trending, aseismic Cocos Ridge, which is interpreted as the trace of a hot spot (e.g., Walther 2003). The entire Cocos Ridge is more than 1000 km long, 250–500 km broad, and rises ca. 2 km above the ocean floor. The timing of the onset of ridge subduction is still in debate. Abratis and Wörner (2001) assume that the Cocos Ridge has been subducting since 8 Ma, whereas other studies propose a much younger history, depending on the method used: 3.6 Ma (Collins *et al.* 1995) and 3–2 Ma (MacMillan *et al.* 2004). The studies of Morell *et al.* (2012), Gardner *et al.* (2013), and Lonsdale and Klitgord (1978) support the assumption that the front edge of the ridge arrived at the trench later than 3 Ma. In the most recent modeling study, Zeumann and Hampel (2015) derive an onset of Cocos Ridge subduction at ~2 Ma.

The Limón back-arc basin belongs to the southern Central American arc-trench system and is situated beneath the present-day coastal plain and continental shelf of eastern Costa Rica (Fig. 3). Its northern boundary is the Hess Escarpment. To the west and to the south the basin is fronted by the volcanic arc. The eastward extent is defined by the 200 m bathymetric contour line of the Caribbean Sea and by the extent of the Limón fold-and-thrust belt, respectively (Fig. 3). The fill of the Limón Basin consists of Upper Cretaceous to Pleistocene deep marine to continental volcaniclastic rocks (Sheehan and Penfield 1990; Coates *et al.* 1992; Amann 1993; Bottazzi *et al.* 1994; Fernandez *et al.* 1994; McNeill *et al.* 2000; Mende 2001; Campos 2001; Coates *et al.* 2003) (Fig. 4). Deposition of shallow-water carbonates occurred during Late Cretaceous, Eocene and Oligocene times on local structural highs. The Limón Basin can be subdivided into a northern and a southern sub-basin, separated by the E-W trending Trans-Isthmic Fault System.

2.1. Geology and Stratigraphy of the Limón Back-Arc Basin

The South Limón Basin contains approx. 6–10 km-thick sedimentary rocks that were deformed by NE-directed folding and thrusting during the Late Neogene (Bottazzi *et al.* 1994; Mende 2001). The resulting fold-and-thrust belt is called the South Limón fold-and-thrust belt in this study. Stratigraphic information for the South Limón Basin is based on onshore outcrops and well data. The oldest sediments consist of ~1280 m-thick pelagic limestones and intercalated volcaniclastic rocks of Late Campanian to Maastrichtian age (Changuinola Formation, Fig. 1). The Changuinola Formation is overlain by up to 3000 m-thick Paleocene to Lower Eocene, coarse-grained, volcaniclastic turbidites, debris flow deposits, lava flows and tuffs of the Tuís Formation, which represent a prograding deepwater apron system (Mende 2001). An early contractional deformation phase during Eocene to Oligocene times resulted in the uplift of the Moín High (Brandes *et al.* 2009) and the formation of significant tectonic and topographic relief, as implied by the coeval deposition of 150-200 m-thick shallow-water limestones of the Las Animas Formation on local structural highs (Amann 1993; Mende 2001), and of 700–900 m-thick hemipelagic mudstones, calcareous turbidites, and carbonate debris flow deposits of the Senosri Formation in adjacent basin areas (Mende 2001). During the Late Oligocene a basin-wide unconformity formed, probably caused by uplift of the island arc in combination with a major sea-level fall (Seyfried *et al.* 1991; Amann 1993; Krawinkel *et al.* 2000). Subsequently, carbonate ramps built up on top of the uplifted areas. These carbonate ramps are overlain by up to 2000 m-thick shallow-water volcaniclastic sediments of the Upper Oligocene to Upper Miocene Uscari Formation, interpreted as delta-influenced shelf deposits (Amann 1993; Mende 2001). The Uscari Formation is overlain by the shallow-water limestones and volcaniclastic rocks of the 400–1800 m-thick Río Banano Formation (Amann 1993; Bottazzi *et al.* 1994; Mende 2001). The South Limón fold-and-thrust belt developed in the Neogene. On the fold belt, wedge-top basins formed (Brandes *et al.* 2007a), which were filled by shallow marine and

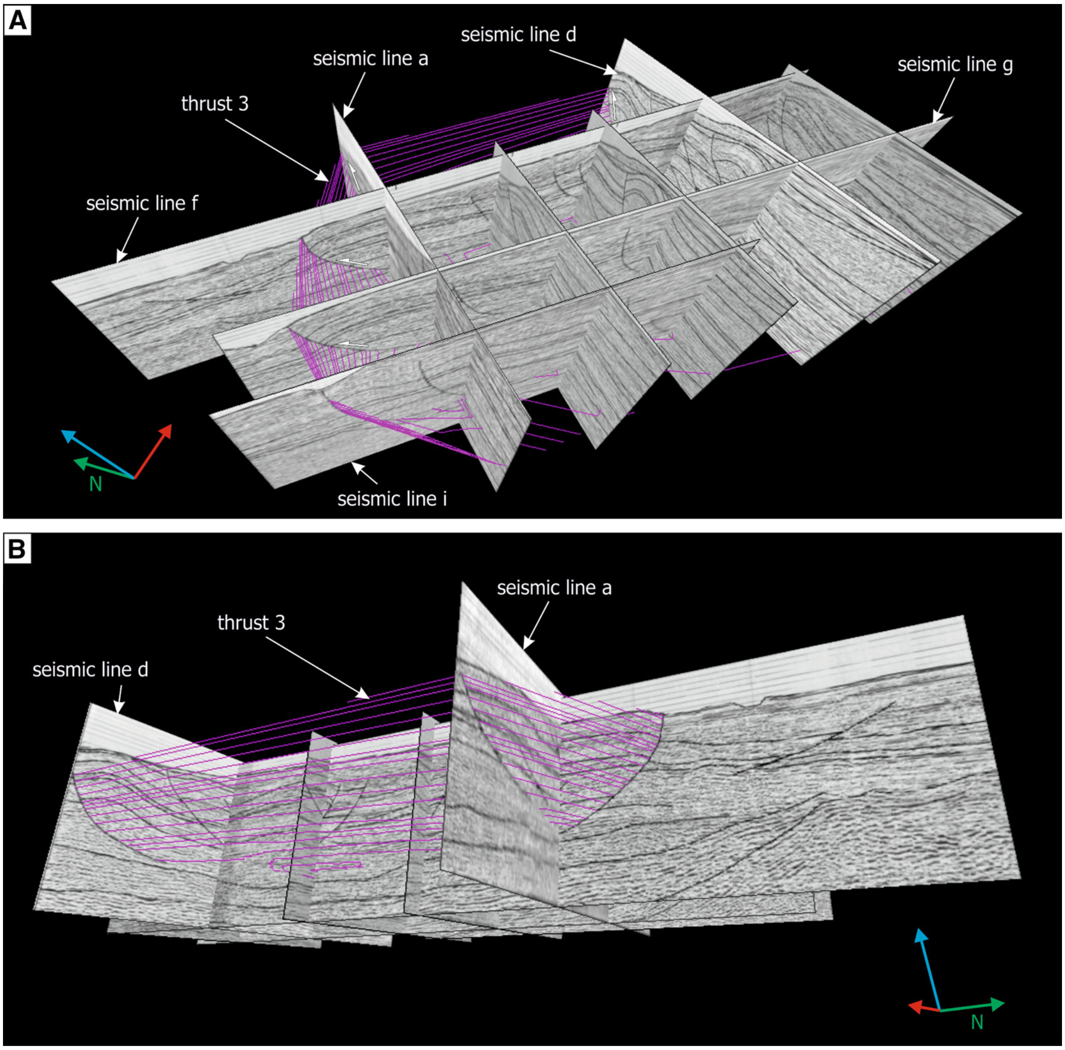

Figure 4
Construction of the 3-D model using the 2-D seismic reflection lines. All thrust traces from the individual seismic sections form a prominent bend in the fold-and-thrust belt. The thrusts were linearly splined to form 3-D fault surfaces. The fault surface of thrust 3 is shown as a set of isolines

continental deposits of the Plio-Pleistocene Suretka Formation (Amann 1993; Bottazzi *et al.* 1994; Mende 2001).

3. Database and Methods

This study is based on nine two-dimensional seismic reflection lines that were acquired during onshore and offshore campaigns in the 1970s and 1980s and made available by the Costa Rican Ministry of Environment and Energy (MINAE) (Fig. 2). Stratigraphic and lithological information for the seismic interpretation was derived from well 1 located close to the NE–SW-trending seismic sections and well 2 on the top of the Moín High (Fig. 2). The latter well penetrates Pleistocene to Miocene sandstones, shales, and limestones. To correlate the major reflectors on the five NE–SW-trending sections (lines a–e), four NW–SE-trending cross-lines (lines f–i) were used. The interpretation of the seismic sections has been presented by Brandes *et al.* (2007c).

3.1. Model Building

We constructed a 3-D subsurface model in the software package 3DMove™ by placing the seismic sections in their correct geographical positions (Fig. 4a, b) and interpolating traces of stratigraphic horizons and their cutoffs at faults. The model contains three major listric thrust faults, which we name, from the trailing- to the leading-edge, thrusts 1, 2 and 3, respectively. In Fig. 4a, b we show, based on thrust 3, how the thrust traces from the individual seismic sections form the prominent bend in the fold-and-thrust belt. The thrusts were first linearly splined to form 3-D fault planes and then the traces of three stratigraphic horizons (base Pleistocene and two intra Miocene reflectors) were taken from the interpretation and meshed into 3-D surfaces with a spline algorithm. The limited coverage of seismic data caused a small triangular hole (approx. 2 km edge length) in the model (Fig. 5a1 and a4). However, this did not negatively affect the modeling. The resulting 3-D structural model was consistent and robust for all further analysis.

All faults detach at one level, at ca. 5 km depth below sea level. The detachment depth is controlled by a lithological contrast between the underlying platform carbonates of the Senosri Formation and the incompetent shales of the Uscari Formation Brandes *et al.* (2007b, c). Above all thrust faults, hanging-wall anticlines were developed (Fig. 5b). These structures can be classified as fault-propagation folds (Suppe and Medwedeff 1990; Brandes and Tanner 2014), based on: (a) the offset along the thrusts decreases up-dip of the fault and (b) the position of the anticlines near to the fault tip. They are not fault-bend folds, because the slight bend in, e.g., thrust 1 (Fig. 5b) is minor and could not cause the observed anticline amplitude by pure fault-bend folding.

The structural restoration was performed with 3DMove™, using the fault-parallel flow algorithm (Ziesch *et al.* 2014). This method constructs flow paths for all particles of the hanging wall. The flow paths are at all times parallel to the fault plane in the transport direction. Fault-parallel flow is a suitable approach for thrusts with cutoff angles below 30° (Ziesch *et al.* 2014). With the use of the strain toolbox in Move™, we recorded the dilatation strain history of the stratigraphic horizons in the model during the sequential restoration.

4. Structural Analysis

In map view the traces of the thrust planes in the model are convex to the foreland. In the east the thrusts strike NW–SE and curve to strike NE–SW in the west, i.e. there is a 90° bend in the strike of the thrust planes (Figs. 2, 4, 5a, 6a, b). The seismic lines show that there is displacement on all of the thrusts, as shown by displacements of the seismic reflectors, irrespective of their orientation. Figure 6b shows the along-strike heave on all three thrusts in map view. This illustrates that the maximum heave on all three faults is in the middle of the bend of the fold-and-thrust belt, implying that it is not a lateral/frontal ramp system, but rather a true array of curved faults. Correlating the maximum heave from thrust to thrust gives the vector of the main transport direction (azimuth N018°), which we chose as the transport direction to retro-deform the model.

4.1. Structural Restoration

Based on the match of stratigraphic cutoffs (base Upper Miocene), we first determined the maximum amount of displacement on each of the faults (thrust 1: 800 m; thrust 2: 600 m; thrust 3: 250 m; see Fig. 7). We assumed foreland propagation of the deformation front, i.e. thrust 1 moved first and was followed by thrusts 2 and 3; i.e., each successive thrust was moved by a smaller amount than the previous one.

In 3D-Move™ the fault-parallel flow algorithm can be implemented in 3-D, albeit with a constant transport direction. The structural restoration involved first restoring the hanging wall of fault 3, then that of fault 2, and finally that of fault 1. In each case the footwall and hanging-wall cutoffs of the base Miocene were matched. Throughout the restoration process, we tracked the strain evolution of all hanging-wall objects.

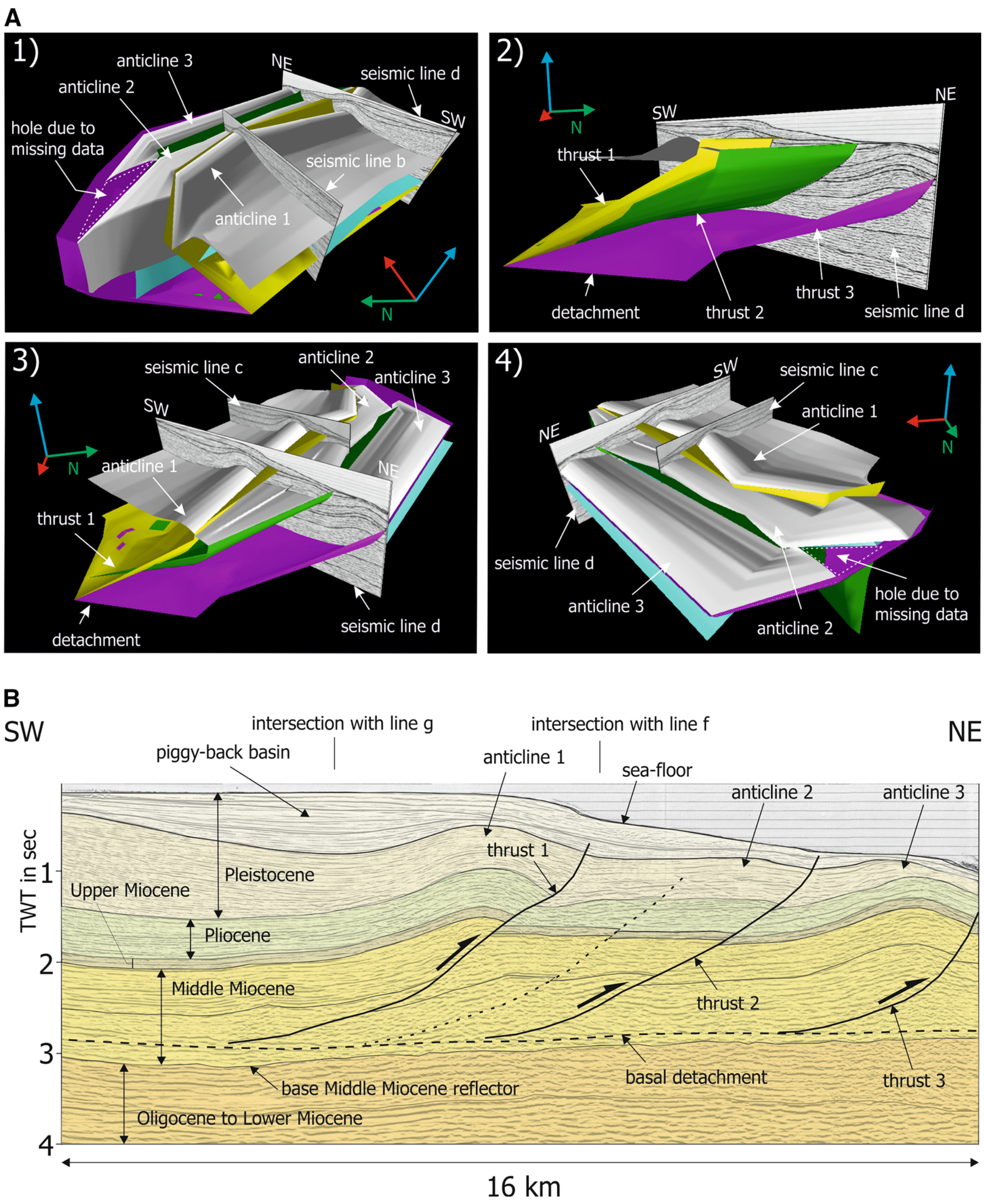

Figure 5

a The bend of South Limón fold-and-thrust belt as 3-D subsurface model in 3D Move^{TM}. The structural model contains three thrusts and their related hanging-wall anticlines. The 2-D traces of three stratigraphic horizons (base Pleistocene and two intra Miocene reflectors) were taken from the interpreted seismic sections and meshed into 3-D surfaces using a spline algorithm. **a**1, **a**4 Due to missing data there is a triangular hole in the model. **b** Interpreted seismic section of the South Limón fold-and-trust belt. The basal detachment lies at the base of the Middle Miocene deposits, controlled by a lithological change from limestones to overlying shales

4.2. Strain Modeling

3-D kinematic modeling can also provide information on the strain distribution within a model. The strain is displayed as an attribute on a stratigraphic surface, in this case the base of the Pleistocene and coded according to color (Fig. 8). We will first

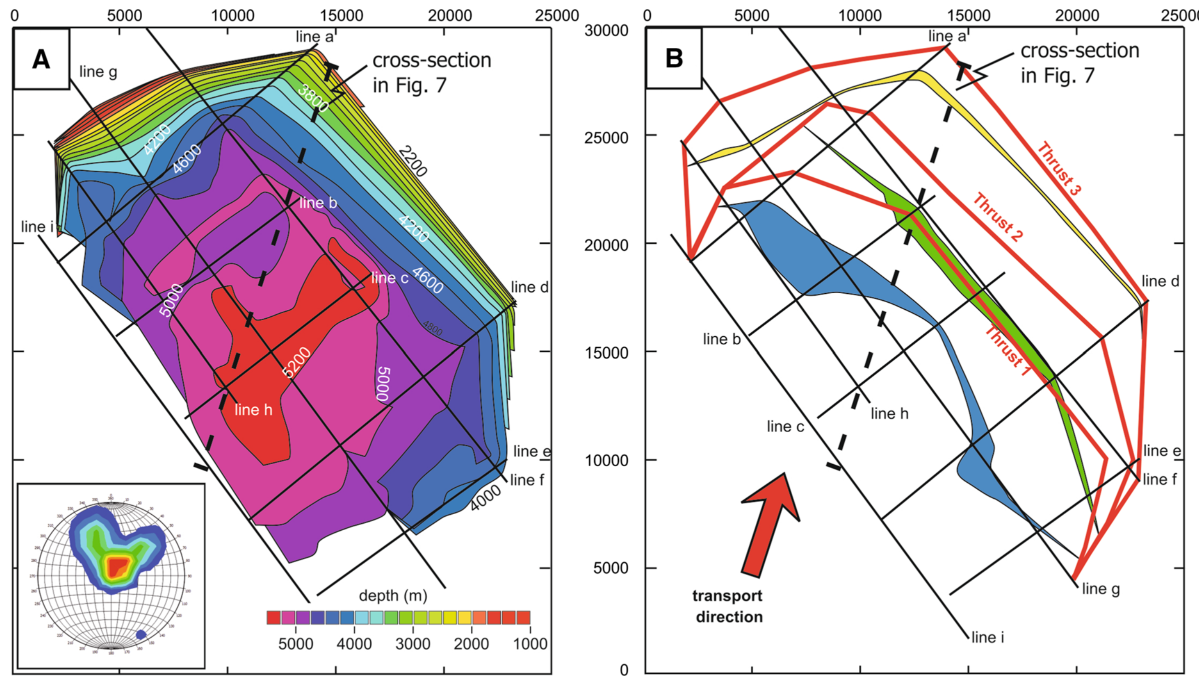

Figure 6

a Isoline map of the basal detachment surface. The detachment has a maximum depth of 5200 m. **b** Heave map for all three thrusts. This map shows that the maximum heave is in the middle of the bend of the fold-and-thrust belt, implying that it is not a lateral-frontal ramp system, but rather a true array of curved faults. Correlating the maximum heave from thrust to thrust gives the vector of the main transport direction (azimuth N018°)

describe the strain history in terms of retro-deformation, in which the youngest fault was retro-deformed first and the oldest fault was retro-deformed last. We invert this sequence to discuss the model in terms of forward deformation. During the retro-deformation, the amount of strain measured is the inverse of that produced during forward deformation. In addition, if the different phases of a strain path are reversed in the correct order (because strain is not commutative), the magnitude of finite strain within any fault block is identical after either retro- or forward deformation.

4.3. Structural Restoration

4.3.1 Thrust 1

Restoration of the leading-edge hanging-wall anticline results in a strain pattern nearly strike-parallel to thrust 1, irrespective of the thrust strike, with an abrupt change at the orogenic bend. Contractional strain is manifested on the forelimb of the hanging-wall anticline, while a zone of dilative strain spreads from the anticline crest to the backlimb (Fig. 8a). Strain magnitudes are 5 % and greater. Not only is the hanging-wall of the active thrust deformed, but it also affects the hanging walls of thrusts 1 and 2. This can be seen especially in the region of the bend, where strain is characterized mainly by extension. A linear ENE-WSW trending zone of dilative strain is the most pronounced element. There are also subordinate, WNW-ESE striking, dilative-strain zones (Fig. 8a).

4.3.2 Thrust 2

During the subsequent retro-deformation step, the strain pattern remains the same as before. However, due to the fact that the spacing between the thrusts is smaller, the strain is further distributed over the second and third hanging-wall anticlines. The dilative strain in hanging-wall anticline 1 follows the trend of

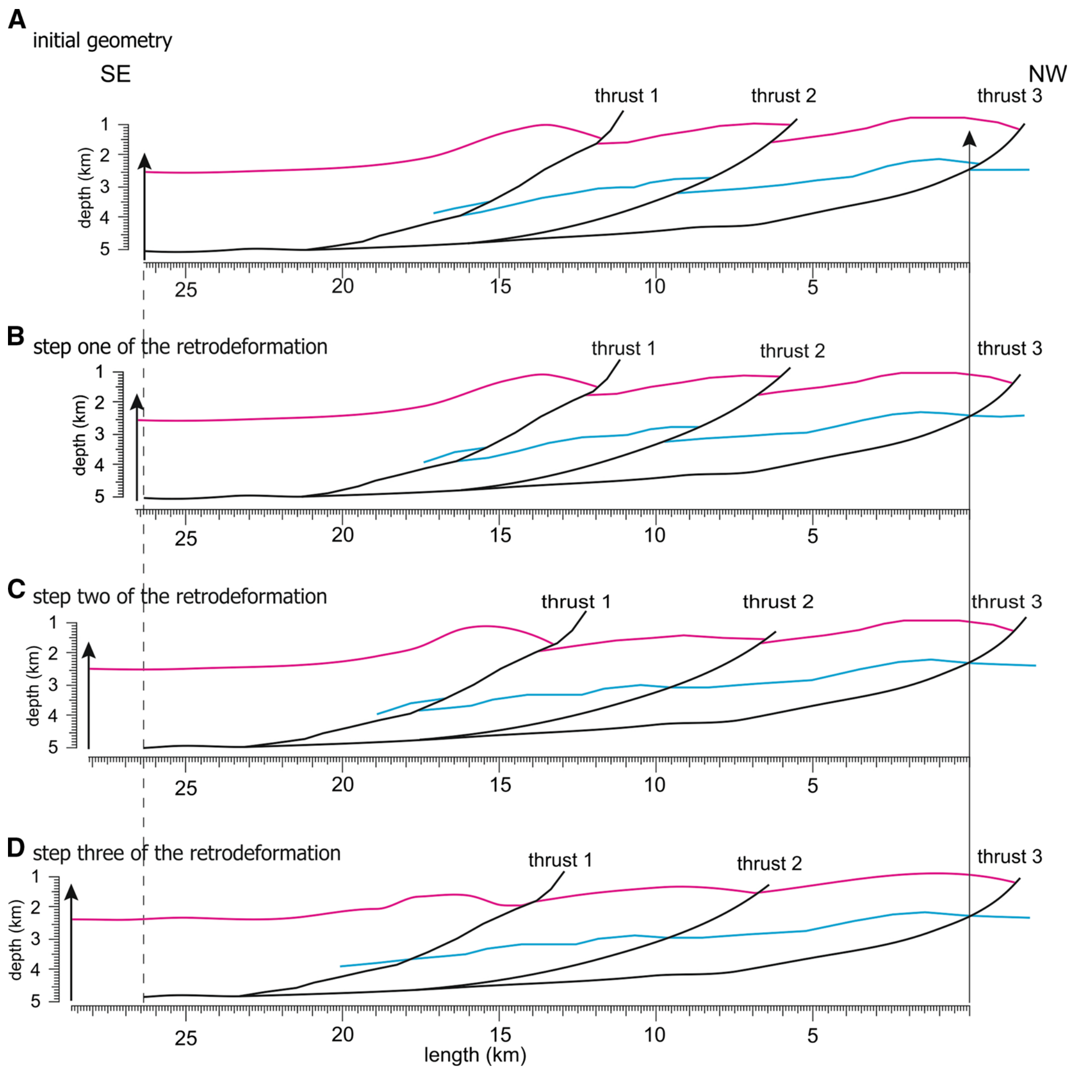

Figure 7

Structural restoration. A cross section (parallel to the transport direction), extracted from the 3-D model (see Fig. 2 for location), showing the present-day situation (**a**) and the three retro-deformation steps (**b–d**). The structural restoration involved first restoring the hanging wall of fault 3, then that of fault 2, and finally that of fault 1. In each case, the footwall and hanging wall cutoffs of the base of the Miocene were matched. Based on the structural restoration we estimate a horizontal shortening of 9 %, see Table 1 for shortening derived from the individual retro-deformation steps

Table 1

Shortening of the cross section shown in Fig. 7

	Length (in km)	Shortening (in km)	Shortening (in %)
Present-day	26.3		
Step 1	26.6	0.3	1.14
Step 2	28.1	1.8	6.84
Step 3	28.7	2.4	9.13

Step one after restoration of thrust 3, *step two* after restoration of thrust 2, *step three* after restoration of thrust 1

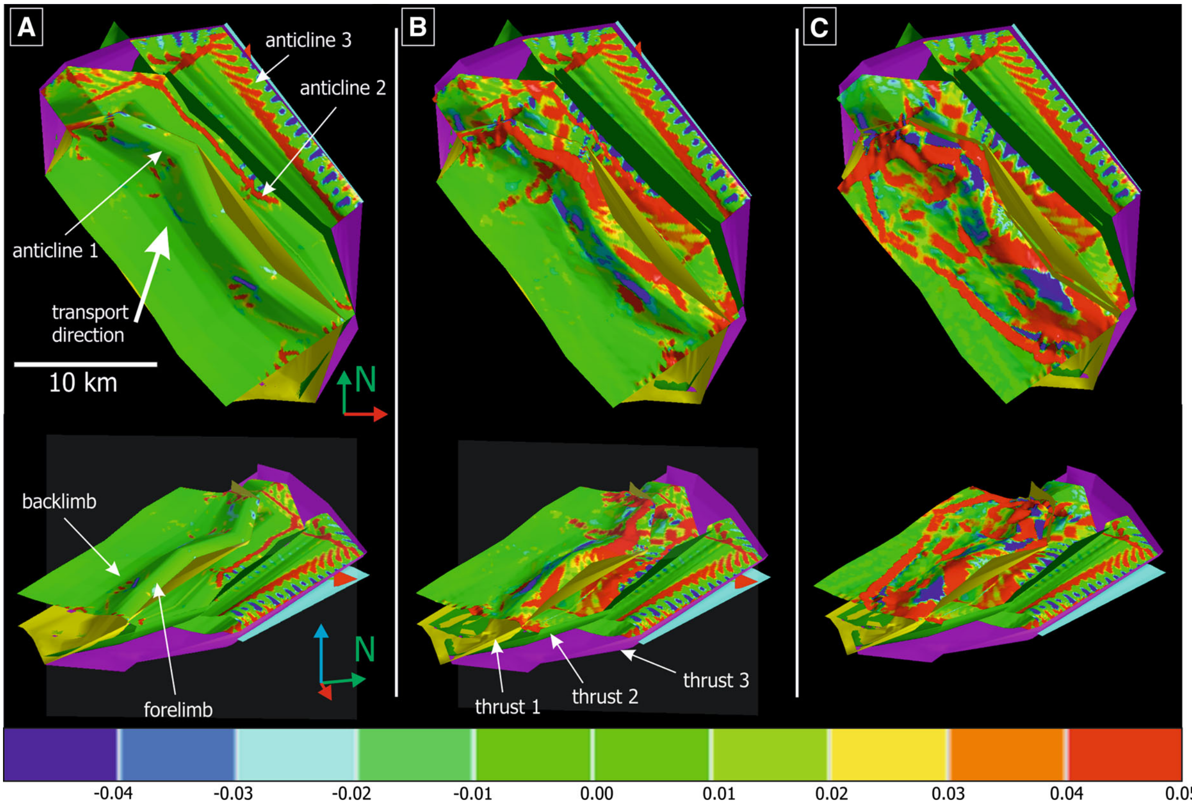

Figure 8

Strain distribution within the South Limón fold-and-thrust belt. **a** Situation after the restoration of thrust 3. **b** Situation after the restoration of thrust 2. **c** Situation after the restoration of thrust 1. The strain is displayed as a *color-coded attribute* on the base Pleistocene horizon, with dilative strain in *red* and contractional strain in *blue*. *Green colors* indicate low to zero strain. Strain values are dimensionless. The strain history is shown in terms of retro-deformation, in which the youngest fault was retro-deformed first and the oldest fault was retro-deformed last. The strain modeling shows contractional deformation concentrated on the forelimbs of the anticlines, whereas dilative deformation characterizes the anticlinal crests and backlimbs. As a result of the close thrust spacing strain not only affects the hanging-wall anticline of the active thrust, but also the hanging walls above it. The strain distribution in the bend area is similar to the general pattern in the hanging-wall anticlines and follows the same trend as the orogenic bend, i.e. from NW–SW in the west to SW–NE in the east

the hinge line (Fig. 8b). Strong modifications of the strain distribution occur in the bend. Previous ENE-WSW striking zones of dilative strain are now overprinted by dilative N–S trending strain zones.

4.3.3 Thrust 3

In this step, the strain pattern in hanging-wall anticline 3 drastically changes and increases. Zones of dilative strain parallel to the former hinge line are dissected and strongly replaced by anastomosing zones of contractional strain, as indicated by the blue colors (Fig. 8c). This affects the whole backlimb of hanging wall 3 up to 10 km from the front of thrust 1. Strain zones in the bend are more curvilinear and thicker than in Fig. 8b.

5. Discussion

All seismic lines, irrespective of their orientation to the bend, show that there is displacement on all the thrusts. Following this observation, the structural modeling was carried out with a tectonic transport direction to the NNE that bisects the two major strike directions of the thrusts. The retro-deformation produced reasonable geometries once the fault slip was restored. With this one direction we produce a reasonable restoration of the 3-D model, which indicated the validity of our method. This implies that the assumption of a NNE-directed transport in the bend area is suitable to explain the structural evolution, i.e., it is a primary arc (in the terms of Hindle and Burkhard 1999). This interpretation is supported by the heave map (Fig. 6b); for example, in that heave on thrust 3 is nearly constant parallel to strike (around the bend of the fold-and-thrust belt). Our modeling shows this part of the offshore South Limón fold-and-thrust belt, with the bend to the northwest, probably evolved in one single deformation phase. Therefore, it is not an orocline in the sense of Carey (1955, 1958).

Analyzing salients (Gray and Stamtakos 1997; Mukul and Mitra 1998) and syntaxes (Butler *et al.* 1989; Gates *et al.* 2004) is an important step toward understanding the geodynamics of fold-and-thrust belts (Poblet and Lisle 2011). In many cases curved fold-and-thrust belts are regarded as oroclines, such as the Patagonian-Fuegian Andes (Dalziel and Elliot 1973) and the Cantabrian Arc (Gutiérrez-Alonso *et al.* 2012). The curved Panama Deformed Belt in the southeast part of the South Limón fold-and-thrust belt has been considered an orocline with three main deformation stages (Montes *et al.* 2012). Marshak (2004) showed that curvatures of fold-and-thrust belts can be caused by the interaction of the propagating belt with subsurface obstacles. Based on this model, Brandes *et al.* (2007c, 2009) proposed that bending of the thrust planes was the result of the interaction of the northwestward-propagating fold-and-thrust belt with the Moín basement high in the subsurface (Figs. 1, 2).

The South Limón fold-and-thrust belt has been interpreted as the western prolongation of the North Panama deformed belt (Silver *et al.* 1990; Goes *et al.* 1993). The latter was caused by the collision of Panama with South America around 25–23 Ma (Farris *et al.* 2011). Using a basin modeling study, Brandes *et al.* (2008) showed that the subsidence in the South Limón basin increased at around 23 Ma, which may indicate the onset of fold-and-thrust belt formation in the back-arc. This fits the data of Farris *et al.* (2011).

A transition from marine to continental deposits occurred at the end of the Late Miocene. During the Plio-Pleistocene wedge-top basins were filled with coarse alluvial sediments (Suretka Formation). These deposits contain granodiorite clasts derived from the rising Talamanca Range (Amann 1993). Young and ongoing deformation is indicated by strongly tilted deposits of the Suretka Formation in the Río Cerere (Amann 1993), the recent opening of the Bocas del Toro Bay (Greb *et al.* 1996) and the 1991 Limón earthquake (Protti and Schwartz 1994). Morell (2016) postulates that Cocos Ridge subduction is the first-order driver for the South Limón fold-and-thrust belt, based on the supposition that shortening decreases eastwards. However, we speculate that this decrease in the shortening could also be a function of the bend in the fold-and-thrust belt that we describe here.

Following Marshak (2004), the curvature of fold-and-thrust belts can be also the result of an interaction with strike-slip faults. A NNE-directed tectonic transport of the South Limón fold-and-thrust belt requires a left-lateral strike-slip zone to compensate the movements and thereby decoupling the South Limón fold-and-thrust belt from the North Costa Rican arc segment.

For the South Limón fold-and-thrust belt transport-parallel simple shear can be ruled out, because the offset along the thrusts is mainly constant even along strike of the bend. Based on the model of Ferrill and Groshong (1993), uniform displacement/uniform shortening (NNE directed in the bend and NE directed in the main part of the fold belt) would be therefore a suitable kinematic classification for the South Limón fold-and-thrust belt.

5.1. Implications for the Geology of Costa Rica

There is a left-lateral fault zone in central Costa Rica; the so-called Trans-Isthmic fault system that has been analyzed over the last 25 years by studies that argue for (Seyfried *et al.* 1991; Krawinkel and Seyfried 1994; Marshall and Fisher 2000) and against (Fernández Arce 1996), both its presence and kinematic timing. Some authors have interpreted the Trans-Isthmic fault system as an old structure that was already present during the early stages of island-arc evolution (Seyfried *et al.* 1991).

From the seismic lines it is evident that there is displacement on all of the thrusts, irrespective of their orientation. To allow movements in the structural modeling that were evenly distributed on all thrusts, we believe a transport direction that bisects the two major strike directions of the thrusts is required, and therefore we chose an azimuth of N018° for the thrust transport vector. This transport direction is almost identical to the plate vector of the Cocos Plate, as shown by Naif *et al.* (2013; Fig. 2). The results show that our modeling is able to correctly restore the 3-D geometry of the South Limón fold-and-thrust with a single NNE-directed tectonic transport. Such a transport requires a left-lateral strike-slip zone that decouples the fold-and-thrust belt from the North Costa Rican arc segment and indicates that the Trans-Isthmic fault system must be present at this time. The results of our modeling are consistent with the model of Fan *et al.* (1993), where the South Limón fold-and-thrust belt interacts with a diffuse east–west trending, left-lateral strike-slip zone in the area of Puerto Limón and fits fault plane solutions from Marshall and Fisher (2000; Fig. 2) that imply that the back-arc thrusting is compensated inland along the Trans-Isthmic fault system by strike-slip motion.

Further evidence for the presence of the Trans-Isthmic fault system can be found in the work of Pindell and Kennan (2009) where lateral escape tectonics in Panama is postulated that also require an east–west trending fault zone in Costa Rica.

5.2. *Implications for Subseismic-Scale Deformation Structures*

In many fold-and-thrust belts, subseismic-scale deformation structures are manifested as fracture sets. The curvature of anticlines is a proxy for fracture density (Lisle 1994; Fisher and Wilkerson 2000). Therefore, the analysis of strain distribution over time (Fig. 8) has the potential to predict the fracture distribution within the analyzed part of the South Limón fold-and-thrust belt. In general, this modeling shows contractive strain of the forelimbs and dilative strain on the backlimbs of the hanging-wall anticlines. The contraction in a narrow strip on the leading edge of each hanging-wall anticline partially changes into dilative strain on the anticlinal crests. The final step (i.e. after the restoration of the whole model) shows that both contractional and extensional strain zones exist as a tiled pattern (Fig. 8c). This is a result of the curvilinear nature of the hinge of anticline 1. Note that although strain in anticlines 2 and 3 is limited to the limbs, the strain of anticline 1 transgresses the hinge line, which might be caused by pronounced listric geometry of the thrust 1. We suggest that mean strains above 4 % are likely to cause permanent brittle deformation (van der Pluijm and Marshak 2004; Lohr *et al.* 2008). Furthermore, we propose that the strain distribution can be interpreted as a direct proxy for fracture intensity (Lisle 1999; Lohr *et al.* 2008).

6. *Conclusions*

The evolution of the bend in the South Limón fold-and-thrust belt can be modeled with a simple NNE-directed transport, implying one deformation phase, i.e., the bend is not an orocline, but rather a primary arc. The pronounced bend is most likely an effect of the interaction of the fold belt with the Trans-Isthmic fault system and the Moín basement high in the subsurface. The strain modeling shows contractional deformation concentrated on the fore-limbs of the anticlines, whereas dilative deformation focuses on the anticlinal crests and backlimbs. Due to the close thrust spacing, strain not only affects the respective hanging-wall anticline of the active thrust, but also the ones above it. The strain distribution in the bend area is similar to the strike of the hanging-wall anticlines and follows the trend of the bend.

Acknowledgments

We are grateful to W. Bandy for the opportunity to contribute to this volume and his editorial comments. We thank H. Seyfried and two anonymous reviewers for thoughtful and encouraging remarks. We would like to thank the Costa Rican Ministry of Environment and Energy (MINAE) for providing the seismic data. Midland Valley is gratefully thanked for an academic license for Move^{TM}.

References

Abratis, M., and Wörner, G. (2001), *Ridge collision, slab-window formation, and the flux of Pacific asthenosphere into the Caribbean realm*, Geology *29*, 127–130. doi:10.1130/0091-7613(2001)029<0127:RCSWFA>2.0.CO;2.

Affolter, T., and Gratier, J.-P. (2004), *Map view retrodeformation of an arcuate fold-and thrust belt: The Jura case,* Journal of Geophysical Research *108*, B03404. doi:10.1029/2002JB002270.

Amann, H. (1993), *Randmarine und terrestrische Ablagerungsräume des neogenen Inselbogensystems in Costa Rica (Mittelamerika)*, Profil *4*, 161 pp.

Argand, E. (1924), *La tectonique de l'Asie*, 13th International Geological Congress Conf. Proceedings, Brussels, pp. 171.

Astorga, A., Fernandez, J.A., Barboza, G., Campos, L., Obando, J., Aguilar, A., and Obando, L.G. (1991), *Cuencas sedimentarias de Costa Rica: evolucion geodinamica y potencial de hidrocarburos*, Revista Geologica de América Central *13*, 25–59.

Barboza, G., Fernández, A., Barrientos, J., and Bottazzi, G. (1997), *Costa Rica: Petroleum geology of the Caribbean margin,* Leading Edge *16*, 1787–1794.

Barckhausen, U., Ranero, C.R., von Huene, R., Cande, S.C., and Roeser, H.A. (2003), *Revised tectonic boundaries in the Cocos Plate off Costa Rica: Implications for the segmentation of the convergent margin and for plate tectonic models*, Journal of Geophysical Research *106*, 19207–19220. doi:10.1029/2001JB000238.

Bottazzi, G., Fernandez, A. and Barboza, G. (1994), Sedimentología e historiatectono-sedimentaria de la cuenca Limón Sur. In Seyfried H. & Hellmann W. (eds.) Geology of an Evolving Island Arc, The Isthmus of Southern Nicaragua, Costa Rica and Western Panamá, Profil 7, pp. 351–389.

Bowland, C.L. (1993), *Depositional history of the western Colombian Basin, Caribbean Sea, revealed by seismic stratigraphy*. GSA Bulletin *105*, 1321–1345. doi:10.1130/0016-7606(1993)105<1321:DHOTWC>2.3.CO;2.

Brandes, C., and Tanner, D.C. (2014), *Fault-related folding: a review of kinematic models and their application*, Earth Science Reviews *138*, 352–370. doi:10.1016/j.earscirev.2014.06.008.

Brandes, C., Astorga, A., and Winsemann, J. (2009), *The Moín High, East Costa Rica: Seamount, laccolith or contractional structure?* Journal of South American Earth Sciences *28*, 1–13. doi:10.1016/j.jsames.2009.02.005.

Brandes, C., Astorga, A., Littke, R., and Winsemann, J. (2008), *Basin modelling of the Limón Back-arc Basin (Costa Rica): burial history and temperature evolution of an island-arc related basin system,* Basin Research *20*, 119–142. doi:10.1111/j.1365-2117.2007.00345.x.

Brandes, C., Astorga, A., Back, S., Littke, R., and Winsemann, J. (2007), *Fault controls on sediment distribution patterns, Limón Basin, Costa Rica,* Journal of Petroleum Geology *30*, 25–40. doi:10.1111/j.1747-5457.2007.00025.x.

Brandes, C., Astorga, A., Back, S., Littke, R., and Winsemann, J. (2007), *Deformation style and basin-fill architecture of the offshore Limón Back-arc basin*, Marine and Petroleum Geology *24*, 277–287. doi:10.1016/j.marpetgeo.2007.03.002.

Brandes, C., Astorga, A., Blisniuk, P., Littke, R., and Winsemann, J. (2007), Anatomy of anticlines, piggy-back basins and growth strata: a case study from the Limón Fold-and-thrust belt, Costa Rica. In: Nichols, G., Williams, E., and Paola, C. (eds) Sedimentary Processes, Environments and Basins: A Tribute to Peter Friend, IAS Special Publication *38*, pp. 91–110, Blackwell Science, Oxford. doi:10.1002/9781444304411.ch5.

Butler, R.W.H., Prior, D.J., and Knipe, R.J. (1989), *Neotectonics of the Nanga Parbat Syntaxis, Pakistan, and crustal stacking in the northwest Himalayas,* Earth and Planetary Science Letters *94*, 329–343. doi:10.1016/0012-821X(89)90150-7.

Campos L. (2001), *Geology and basins history of middle Costa Rica: an intraoceanic island arc in the convergence between the Caribbean and the central pacific plates,* Tübinger Geowissenschaftliche Arbeiten, Reihe A *62*, 138 pp.

Carey, S.W. (1958), A tectonic approach to continental drift. In: Carey, S.W. (ed) Continental Dift: A symposium, Tasmania, Hobart, pp. 177–355.

Carey, S.W. (1955), *The orocline concept in geotectonics*, Proceedings Royal Society Tasmania *89*, 255–288.

Coates, A.G., Aubry, M-P., Berggren, W.A., Collins, L.S. and Kunk, M. (2003), *Early Neogene history of the Central American arc from Bocas del Toro, western Panama*. GSA Bulletin *115*, 271–287.

Coates, A.G., Jackson, J.B.C., Collins, L.S., Cronin T.M., Dowsett, H.J., Bybell, L.M., Jung, P. and Obando, J.A. (1992), *Closure of the Isthmus of Panama: The near-shore marine record of Costa Rica and western Panama*. GSA Bulletin *104*, 814–828.

Cooper, M.A., and Trayner, P.M. (1986), *Thrust-surface geometry: Implications for thrust-belt evolution and section-balancing techniques*, Journal of Structural Geology *8*, 305–312. doi:10.1016/0191-8141(86)90051-9.

Collins, L.S., Coates, A.G., Jackson, J.B.C., and Obando, J.A. (1995), Timing and rates of emergence of the Limón and Bocas del Toro basins: Caribbean effects of Cocos Ridge subduction? In: Mann, P. (ed) Geologic and Tectonic Development of the Caribbean Plate Boundary in Southern Central America, Geological Society of America Special Paper *295*, pp. 263–289. doi:10.1130/SPE295-p263.

Corrigan, J., Mann, P., and Ingle, Jr, J.C. (1990), *Forearc response to subduction of the Cocos Ridge, Panama-Costa Rica,* GSA Bulletin *102*, 628–652. doi:10.1130/SPE295-p263.

Dahlstrom, C.D.A. (1969), *Balanced cross sections,* Canadian Journal of Earth Sciences *6*, 743–757. doi:10.1139/e69-069.

Dahlstrom, C.D.A. (1990), *Geometric constraints derived from the law of conservation of volume and applied to evolutionary models for detachment folding,* AAPG Bulletin *74*, 336–344.

Dalziel, I.W.D. and Elliot, D.H. (1973), The Scotia Arc and Antarctic margin. In: Nairn, A.E.M., and Stehli, F.G. (eds) The Ocean Basins and Margins, vol. 1: The South Atlantic. New York, Plenum Press, 171–245. doi:10.1007/978-1-4684-3030-1_5.

DeMets, C. (2001), *A new estimate for present-day Cocos-Caribbean plate motion: Implications for slip along the Central American volcanic arc,* Geophysical Research Letters *28*, 4043–4046. doi:10.1029/2001GL013518.

DePaor, D.G. (1988), *Balanced section in thrust belts part 1: construction,* AAPG Bulletin *72*, 73–90. doi:10.1306/703C81CD-1707-11D7-8645000102C1865D.

Donnelly, T.W. (1989), Geologic history of the Caribbean and Central America, In: Bally, A.W. and Palmer A.R. (eds) The Geology of North America—An overview, Geological Society of America Special Paper A, pp. 299–321.

Fan, G., Beck, S.L., and Wallace, T.C. (1993), *The seismic source parameters of the 1991 Costa Rica aftershock sequence:*

evidence for a transcurrent plate boundary, Journal of Geophysical Research *98* (B9), 15759–15778. doi:10.1029/93JB01557.

Farris, D.W., Jaramillo, C., Bayona, G., Restrepo-Moreno, S.A., Montes, C., Cardona, A., Mora, A., Speakman, R.J., Glascock, M.D., and Valencia, V. (2011), *Fracturing of the Panamanian Isthmus during initial collision with South America*, Geology *39*, 1007–1010. doi:10.1130/G32237.1.

Ferrill, D.A., and Groshong, R.H. (1993), *Kinematic model for the curvature of the northern Subalpine Chain, France*, Journal of Structural Geology *15*, 523–541. doi:10.1016/0191-8141(93)90146-2.

Fernandez Arce, M. (1996), *Evaluacion del hipotetico sistema de falla transcurrente este-oeste de Costa Rica*, Rev. Geol. Amér. Central. *19/20*, 57–74. doi:10.15517/rgac.v0i19-20.8626.

Fernandez, J., Alvaro, A., Guillermo, B., Bottazzi, G., Campos, L., Obando, J., Tejera, R., Arrieta, L., Barrientos, J., Bustos, I., Escalante, G., Pizarro, D., Valerín, E., Astorga, A., Bolanos, X., Calvo, C., Laurito, C., Rojas, J., and Valerio, A. (1997), Mapa Geológico de Costa Rica, Ministerio del Ambiente y Energía, Costa Rica.

Fernandez, J.A., Bottazzi, G., Barboza, G. and Astorga A. (1994), *Tectónica y estratigrafia de la Cuenca Limón Sur*. Rev Revista Geologica de América Central, Vol. Terremoto de Limón, 15–28.

Fisher, D.M., Gardner, T.W., Sak, P.B., Sanchez, J.D., Murphy, K., and Vannucchi, P. (2004), *Active thrusting in the inner forearc of an erosive convergent margin, Pacific coast, Costa Rica,* Tectonics *23*, TC2007, doi:10.1029/2002TC001464.

Fischer, M.P. and Wilkerson, M.S. (2000), *Predicting the orientation of joints from fold shape: results of pseudo-three-dimensional modeling and curvature analysis*, Geology *28*, 15–18. doi:10.1130/0091-7613(2000)28<15:PTOOJF>2.0.CO;2.

Gardner, T.W., Fisher, D.M., Morell, K.D., and Cupper, M.L. (2013), *Upper-plate deformation in response to flat slab subduction inboard of the aseismic Cocos Ridge, Osa Peninsula, Costa Rica,* Lithosphere *5*, 247–264. doi:10.1130/L251.1.

Gates, A.E., Valentino, D.W., Chiarenzelli, J.R., Solar, G.S., and Hamilton, M.A. (2004), *Exhumed Himalayan-type syntaxis in the Grenville orogen, northeastern Laurentia*, Journal of Geodynamics *37*, 337–359. doi:10.1016/j.jog.2004.02.011.

Goes S.D.B., Velasco A.A., Schwartz S.Y., and Lay T. (1993), *The April 22, 1991, Valle de la Estrella, Costa Rica (Mw = 7.7) earthquake and its tectonic implications: a broadband seismic study,* Journal of Geophysical Research *98*, B5, 8127–8142. doi:10.1029/93JB00019.

Gray, M.B., and Stamatakos, J. (1997), *New model for evolution of fold and thrust belt curvature based on integrated structural and paleomagnetic results from the Pennsylvania salient,* Geology *25*, 1067–1070. doi:10.1130/0091-7613(1997)025<1067:NMFEOF>2.3.CO;2.

Greb, L., Saric, B., Seyfried, H., Broszonn, T., Brauch, S., Gugau, G., Wiltschko, C., and Leinfelder, R. (1996), *Ökologie und Sedimentologie eines rezenten Rampen-systems an der Karibikküste von Panamá*, Profil *10*, 1–168.

Gutiérrez-Alonso, G., Johnston, S.T., Weil, A.B., Pastor-Galán, D., and Fernández-Suárez, J. (2012), *Buckling an orogen: The Cantabrian Orocline*, GSA Today *22*, 4–8. doi:10.1130/GSATG141A.1.

Hindle, D., and Burkhard, M. (1999), *Strain displacement and rotation associated with the formation of curvature in fold belts; the example of the Jura arc,* Journal of Structural Geology *21*, 1089–1101. doi:10.1016/S0191-8141(99)00021-8.

Krawinkel, H., Seyfried, H., Calvo, C. and Astorga, A. (2000), *Origin and inversion of sedimentary basins in southern Central America.* Zeitschrift für Angewandte Geologie SH *1*, 71–77.

Krawinkel, J., and Seyfried, H. (1994), A review of plate-tectonic processes involved in the formation of the southwestern edge of the Caribbean Plate, In: Seyfried, H., and Hellmann, W. (eds) Geology of an Evolving Island Arc, The Isthmus of Southern Nicaragua, Costa Rica and Western Panamá, Profil *7*, 47–61.

Lisle, R. (1994), *Detection of abnormal strains in structures using Gaussian curvature analysis*, American Association of Petroleum Geologists Bulletin *78*, 1811–1819.

Lisle, R. (1999), *Predicting patterns of strain from three-dimensional fold geometries: neutral surface folds and forced folds*, Geological Society London, Special Publications *169*(1), 213–221. doi:10.1144/GSL.SP.2000.169.01.16.

Lonsdale, P., and Klitgord, K. (1978), *Structure and tectonic history of the eastern Panama Basin,* GSA Bulletin *89*, 981–999.

Lohr, T., Krawczyk, C.M., Oncken, O., Tanner, D.C., Samiee, R., Endres, H., Thierer, P., Trappe, H., Bachmann, R., and Kukla, P.A. (2008), *Prediction of subseismic faults and fractures: Integration of three-dimensional seismic data, three-dimensional retro-deformation, and well data on an example of deformation around an inverted fault,* AAPG Bulletin *92/4*, 473–485. doi:10.1306/11260707046.

Macedo, J., and Marshak, S. (1999), *Controls on the geometry of fold-and-thrust belt salient*, GSA Bulletin *111*, 1808–1822. doi:10.1130/0016-7606(1999)111<1808:COTGOF>2.3.CO;2.

MacMillan I., Gans P.B., and Alvarado G. (2004), *Middle Miocene to present tectonic history of the southern Central American Volcanic Arc,* Tectonophysics *392*, 325–348. doi:10.1016/j.tecto.2004.04.014.

Marshak, S. (2004), Salients, recesses, arcs, oroclines, and syntaxes – a review of ideas concerning the formation of map-view curves in fold-thrust belts. In: McClay, K.R. (ed) Thrust Tectonics and Hydrocarbon Systems, American Association of Petroleum Geologists, Memoir *82*, pp. 131–156.

Marshall, J.S., Fisher, D.M., and Gardner T.W. (2000), *Central Costa Rica deformed belt: kinematics of diffuse faulting across the western Panama block,* Tectonics *19*, 468–492. doi:10.1029/1999TC001136.

McNeill, D.F., Coates, A.G., Budd, A.F. and Borne, P.F. (2000), *Integrated paleontologic and paleomagnetic stratigraphy of the Upper Neogene deposits around Limon, Costa Rica: A coastal emergence record of the Central American Isthmus*. GSA Bulletin *112*, 963–981.

Mende A. (2001), *Sedimente und Architektur der Forearc- und Backarc-Becken von Südost-Costa Rica und Nordwest-Panamá*, Profil *19*, 130 pp.

Meschede, M., and Frisch, W. (1998), *A plate tectonic model for the Mesozoic and Early Cenozoic history of the Caribbean Plate,* Tectonophysics *296*, 269–291. doi:10.1016/S0040-1951(98)00157-7.

Montes, C., Bayona, G., Cardona, A., Buchs, D.M., Silva, C.A., Morón, S., Hoyos, N., Ramírez, D.A., Jaramillo, C.A., and Valencia, V. (2012), *Arc-continent collision and orocline formation: Closing of the Central American seaway*, Journal of Geophysical Research *117*, B04105. doi:10.1029/2011JB008959.

Morell, K.D. (2016), Seamount, ridge and transform subduction in southern Central America. Tectonics *35*, 10.1002/2015TC003950.

Morell, K.D., Gardner, T.W., Fisher, D.M., Idleman, B., and Zellner, H. (2013), *Active thrusting, landscape evolution and late Pleistocene sector collapse of Barú Volcano above the Cocos-Nazca slab tear, southern Central America*, GSA Bulletin *125*, 1301–1318. doi:10.1130/B30771.1.

Morell, K.D., Kirby, E., Fisher, D., and van Soest, M. (2012), *Geomorphic and exhumational response of the Central American volcanic arc to Cocos Ridge subduction,* Journal of Geophysical Research *117*, B04409, doi:10.1029/2011JB008969.

Morell, K.D., Fisher, D.M., and Gardner, T.W. (2008), *Inner forearc response to subduction of the Panama fracture zone, southern Central America*, Earth and Planetary Science Letters *265*, 82–95. doi:10.1016/j.epsl.2007.09.039.

Mukul, M., and Mitra, G. (1998), *Finite strain and strain variation analysis in the Sheeprock Thrust Sheet: an internal thrust sheet in the Provo salient of the Sevier Fold-and-Thrust belt, Central Utah,* Journal of Structural Geology *20*, 385–405. doi:10.1016/S0191-8141(97)00087-4.

Naif, S., Key, K., Constable, S., and Evans, R.L. (2013), *Melt-rich channel observed at the lithosphere–asthenosphere boundary,* Nature *495*, 356–359. doi:10.1038/nature11939.

Pindell, J.L., and Kennan, L. (2009), Tectonic evolution of the Gulf of Mexico, Caribbean and northern South America in the mantle reference frame: an update, In: James, K.H., Lorente, M.A., and Pindell, J.L. (eds) The Origin and Evolution of the Caribbean Plate, Geological Society, London, Special Publications *328*, pp. 1–55. doi:10.1144/SP328.1.

Poblet, J., and Lisle, R.J. (eds), (2011), *Kinematic evolution and structural styles of fold- and-thrust belts*, Special Publication of the Geological Society of London *349*. doi:10.1144/SP349.4.

Protti, M., and Schwartz, S.Y. (1994), *Mechanics of back arc deformation in Costa Rica: Evidence from an aftershock study of the April 22, 1991, Valle de la Estrella, Costa Rica, earthquake ($M_w = 7.7$),* Tectonics *13*, 1093–1107. doi:10.1029/94TC01319.

Ranero, C.R., and von Huene, R. (2000), *Subduction erosion along the Middle America convergent margin,* Nature *404*, 748–752. doi:10.1038/35008046.

Ross M.I., and Scotese C.R. (1988), *A hierachical tectonic model of the Gulf of Mexico and the Caribbean region,* Tectonophysics *155*, 139–168. doi:10.1016/0040-1951(88)90263-6.

Sala, P., Pfiffner, O.A., and Frehner, M. (2014), *The Alpstein in three dimensions: fold-and-thrust belt visualization in the Helvetic zone, eastern Switzerland*, Swiss Journal of Geoscience *107*, 177–195. doi:10.1007/s00015-014-0168-6.

Seyfried, H., Astorga, A., Amann, H., Calvo, C., Kolb, W., Schmidt, H., and Winsemann, J. (1991), Anatomy of an evolving island arc: tectonic and eustatic control in the south Central American forearc area. In: MacDonald, D.I.M. (ed.) Sedimentation, Tectonics and Eustacy: Sea-level changes at Active Margins, International Association of Sedimentologists, Special Publication *12*, pp. 273–292. doi:10.1002/9781444303896.ch13.

Sheehan, C.A., Penfield, G.T., and Morales E. (1990), *Costa Rica geologic basins lure wildcatters*. Oil Gas Journal Apr. *30*, 74–79.

Silver E.A., Reed D.L., Tagudin J.E., and Heil D.J. (1990), *Implications of the north and south Panama thrust belts for the origin of the Panama orocline*, Tectonics *9*, 261–281. doi:10.1029/TC009i002p00261.

Sitchler, J.C., Fisher, D.M., Gardner, T.W., and Protti, M. (2007), *Constraints on inner forearc deformation from balanced cross sections, Fila Costena thrust belt, Costa Rica*, Tectonics *26*, TC6012. doi:10.1029/2006TC001949.

Suess, E. (1908), Das Antlitz der Erde. Erster Band, Wien, 778 pp.

Suppe J., and Medwedeff D.A. (1990), *Geometry and kinematics of fault-propagation folding*, Eclogae Geologicae Helvetiae *83*(3), 409–454.

Tanner, D.C., Behrmann, J.H., and Dresmann, H. (2003), *Three-dimensional retro-deformation of the Lechtal Nappe, Northern Calcareous Alps,* Journal of Structural Geology *25*, 737–748. doi:10.1016/S0191-8141(02)00057-3.

Tanner, D.C., Bense, F.A., and Ertl, G. (2011), Kinematic retro-modelling of a cross-section through the Western Irish Namurian Basin. In: Poblet, J., and Lisle, R.J. (eds) Kinematic evolution and structural styles of fold- and-thrust belts, Special Publication of the Geological Society of London *349*, 61–76. doi:10.1144/SP349.4.

van der Pluijm, B.A., and Marshak, S. (2004), Earth Structure. Norton and Company, 656 pp.

von Eynatten, H., Schmidt, H., and Winsemann, J. (1993), Plio-Pleistocene outer arc basins in southern Central America, In: Frostick, L., and Steele, R. (eds) Sedimentation and Tectonics, IAS Special Publication *20*, pp. 399–414. doi:10.1002/9781444304053.ch21.

Walther, C.H.E. (2003), *The crustal structure of the Cocos Ridge of Costa Rica,* Journal of Geophysical Research *108*, 1–21. doi:10.1029/2001JB000888.

Wu, S., Yu, Z., Zhang, R., Han, W., and Zou, D. (2005), *Mesozoic-Cenozoic tectonic evolution of the Zhuanghai area, Bohai-Bay Basin, east China: the application of balanced cross-sections,* Journal of Geophysics and Engineering *2*, 158–168. doi:10.1088/1742-2132/2/2/011.

Zeumann, S., and Hampel, A. (2015), *Deformation of erosive and accretive forearcs during subduction of migrating and non-migrating aseismic ridges: Results from 3D finite-element models and application to the Central American, Peruvian and Ryukyu margins,* Tectonics *34*, 1769–1791. doi:10.1002/2015TC003867.

Ziesch, J., Tanner, D.C., and Krawczyk, C.M. (2014), *Strain associated with the fault-parallel flow algorithm during kinematic fault displacement,* Mathematical Geoscience *46*(1), 59–73. doi:10.1007/s11004-013-9464-3.

(Received May 4, 2015, accepted February 26, 2016, Published online March 17, 2016)